Nonlinear Analyses of a Multicavity Prestressed Concrete Reactor Vessel

B. Ducret, J.-D. Favrod, B. Rebora
IENER, Institute of Energy Economics and Power Engineering, Swiss Federal Institute of Technology, CH-1015 Lausanne, Switzerland

A numerical simulation of the behaviour of a high temperature nuclear reactor pressure vessel will be presented. The following points will be examined :

1) failure modes of the reactor vessel when subject to accidental loads (i.e. pressure increase within the cavities),
2) the behaviour of sealing devices under normal servicing conditions over the life span of the power-station. In particular, the sealing of a cavity closure cap when subject to both pressure and temperature gradients is investigated.

These two types of analysis were accomplished through the aid of mathematical model "TRIDI". The model is based on the finite element method. The isoparametric element family which we employed in our calculations is composed of three-dimensional elements used for concrete simulation, a membrane element for the liner and finally bar and sliding elements.

The model takes into account nonlinearities of concrete,namely,the nonlinearity of the stress-strain law under compression, cracking, the influence of the thermal gradient on mechanical characteristics, as well as thermal creep under alternating temperatures. The parameters of the proposed concrete laws were obtained from experiments, allowing us to have some confidence in the accuracy of the obtained results.

The solution of the equilibrium equation is obtained by two series of iterations for each load-step : the first series defines the instantaneous nonlinear equilibrium; the second the creep deformation.

The most significant results of analyses of a multicavity reactor vessel are presented. This concerns, on one hand, comparison of experimental with computational results of an ultimate load analysis on a pressure vessel model subject to an internal pressure increase. On the other hand, creep results of a cavity sealing system over a period of forty years are presented.

This article illustrates that it is possible to numerically simulate extreme nonlinear behaviour of massive reinforced concrete structures. The needed mathematical models are relatively simple and the parameters are easily obtained experimentally.

1. INTRODUCTION

This article presents a synthesis of experimental and analytical results of studies done on two multicavity prestressed concrete reactor vessels designed by Bonnard & Gardel Cons. Eng. Inc., Lausanne. The first analysis evaluates the short-term safety of a reactor vessel when subject to a pressure increase within the cavities and exposes the failure modes. The second appraises the long-term safety in relation to the rheological behaviour of another reactor vessel when subject to a critical load time-history, jeopardizing the feasibility of the closing device of the cavities. Both vessels examined correspond to high-temperature-helium cooled (HHT) reactors presented in reference [1]. The nonlinear three-dimensional numerical model for the analysis of massive structures used for simulation purposes is the "TRIDI" program [2, 3].

2. STATIC ANALYSIS UNDER RAPID LOADING

2.1 Description

For this particular case and kind of analysis, we simulated numerically a test on a small scale model reactor vessel [4, 5]. The goals of both the testing and calculation were to disclose the behaviour of a prestressed concrete reactor vessel when subjected to an increase of internal pressure up to rupture, in order to define its cracking patterns, the failure load and the corresponding failure mechanism.

Figure 1 shows the reactor vessel. The test model, of scale 1/20, measures 2.40 meters in diameter and is 1.95 meters high. It corresponds to an integrated design of HHT reactor , has three production groups arranged symmetrically with respect to the axis of the reactor vessel. To each group correspond one horizontal turbine cavity and eight vertical cavities. In the same figure applied loads are described.

All elements contributing to the reactor vessel's resistance are simulated, including all prestressing wires, vertical horizontal and annular, and liner. Note that the thickness of the liner has been oversized for constructive purposes in comparison with the full-size reactor vessel. The nonlinear behaviour as well as failure of all materials is modellised [6].

2.2 Results

Figure 2 shows the cracking patterns observed in the experiment. Figure 2a shows plastified zones in the liner. Failure occured under a water pressure of 24 N/mm^2 and was characterized by the failure of some annular prestressing wires and local failure of the liner with loss of pressurizing liquid, which could be related to locally large deformations of the vessel. In figure 3a shaded areas represent plastic zones resulting from computation. In figure 3b computed and observed cracking patterns are superposed (each shaded spot represents a crack with trace parallel to shading lines). Good correlation between computation and experiment is observed. The ultimate load reached numerically and characterized by divergence of the computations, was 21 N/mm^2, i.e. 87 % of the experimental one . The analysis of energy dissipation leads to the identification of three

dominant cracking patterns (fig. 2, dashed lines A,B,C) and then to the failure mechanism : local beam mechanism in the outer wall.

3. RHEOLOGICAL ANALYSIS

3.1 Concrete constitutive model

The proposed model describes the evolution of concrete deformation as a function of time and temperature. Total deformation is decomposed into two parts : instantaneous deformation and time-dependent deformation. Temperature variations influence the instantaneous deformation through both the elasticity modulus and thermal expansion. The thermal effect acts upon time-dependent deformation through the parameters of the rheological laws.

Creep deformation at time t, and referential temperature $T_i = 20°C$, is expressed by the parabolic law :

$$\varepsilon_c(t) = \varepsilon_i \cdot a(T_i) \cdot (t - \tau_i)^n$$

where ε_i is the instantaneous deformation applied at time τ_i $\left(\varepsilon_i = \frac{\sigma_i}{E(20)}\right)$;n and $a(T_i)$ were experimentally established. The total creep deformation is calculated by the superposition principle of elementary creep deformations . Figure 4a illustrates the principle. In order to give a clearer picture only instantaneous and creep deformations are represented. At time t and temperature T_k, the total creep deformation is the algebraic sum of the elementary creep contributions due to the instantaneous creep deformations created by each load "i" :

$$\varepsilon_c(t) = \sum_{i=1}^{p} \left[\varepsilon_i \cdot a(T_k) \cdot (t - \tau_k + \Delta\tau_{i,k})^n\right]$$

where τ_k is the time-origin of T_k; $\Delta\tau_{i,k} = (\tau_k - \tau_i)\left(\frac{a(T_i)}{a(T_k)}\right)^n$ defines a new temporal origin for application of the elementary deformation ε_i to take into account the variation of "a" with temperature.

The thermal effect also affects Young's modulus and hence instantaneous deformation. Poisson's ratio remains constant. Further, strength decreases linearly with temperature.

The shrinkage deformation at time t and temperature T is described by Ulitskii's formula [7] :

$$\varepsilon_s(t) = \varepsilon_s(\infty)\left(1 - e^{-B(T) \cdot t}\right)$$

$\varepsilon_s(\infty)$ and B(T) are established experimentally.

The total deformation is the algebraic sum of the instantaneous deformation (linear or not), of the thermal expansion, of the shrinkage and creep deformations and of the variation in instantaneous deformation due to the alteration of Young's modulus.

3.2 Thermal Laws calibration

Laboratory tests on unsealed samples which were undertaken at the Institute for Structural Analysis (ISTACO) of the Swiss Federal Institute of Technology, provide the numerical values of parameters [8]. Figure 4b illustrates Young's modulus linear relation, ultimate strength with respect to temperature. Figure 4c gives the creep and shrinkage parameters values. Other creep and shrinkage parameters n and $\varepsilon_s(\infty)$ are constant, having the values of .27 and -.0004 respectively. Table 1 regroups experimental and assumed parameters, i.e.: Young's modulus, Poisson's ratio and thermal expansion coefficient,creep parameters, shrinkage parameters, compression and tensile uniaxial strengths.

3.3 Test simulation

Figure 4d represents the numerical simulation of a test done at ISTACO, not used for the determination of creep parameters. The test was performed on a cylindrical specimen stored at ambient air during 530 days. The quasi-totality of shrinkage deformation was accomplished by the end of this period. First of all, the temperature was raised from 20 to 200°C, then the load σ was applied for 92 days until t = 638 days. The creep parameters a, n, are those already defined by calibration testing : a(20) = .22, a(200) = .638, n = .27. The deformation of t = 530 to t = 546 days is only the thermal expansion of the sample. The deformation from t = 546 to t = 638 days is the superposition of expansion, elastic and creep deformations.

3.4 Creep analysis

Creep analysis is relative to a HTR-V reactor vessel, a variation on the HHT vessel. The goal of this analysis was to study a cavity closing system when subjected to extreme loads combining prestressing, thermal gradient and internal pressure.

Figure 5a represents the projected closing system, composed of a concrete plug, which rests on the cavity chamfron and is maintained through the aid of support struts. Cavity sealing is assured by a steel joint situated between the plug and the top of the cavity. Figure 5b shows a detail of the support struts and sealing system.

Finite element discretisation is restricted to 1/18 of the reactor vessel, keeping in mind its symmetries. Only one-half of the plug is discretised;truss elements are used to simulate the 8 support struts. Sliding elements quite similar to springs are used to simulate the inside face of the reactor vessel-plug on the level of the sealing joint. Figures 5c and 5d show the finite element meshes. The total number of elements is 210, the number of degrees of freedom 4179 (3 for each node). Material data are given in table 1.

Loading time-history number 1

Its goal is to study the evolution of force exerted on the plug as function of time. This scenario uses sliding elements for the simulation of the plug-vessel interface. The

assumed load time history (fig. 5e) introduces normal servicing pressure at the age of eight years after plug assembly. Further, no prestress losses are taken into account.

This load history defines the maximum force exerted on the plug before start of normal servicing. This force results from creep under prestress.

Results of this analysis are presented in figure 6a and 6b showing the stress evolution in the crushed plug at times t = 284 days and t = 3010 days. After 8 years the maximum compression stress in the plug is approximately - 16 N/mm^2; the observed tensile zones are related to the thermal gradient between the top and bottom of the plug. Figure 6c specifies the evolution of the stress within each support strut. After 8 years the mean normal force, F, of each support is 2.9 10^6N; the integral of forces exerted on the half-plug are to the order of 2.10^7 N. Figure 5b illustrates the problem faced when removing the plug which occured during this scenario. The releasing force, T, needed in order to unplug the system is proportional to the force F exerted on the support strut.

The conclusion to draw from this scenario is that although the safety of the plug or of the sealing system is not questionable, the blocking forces acting on the plug are such that its removal could be problematical.

Loading time-history number 2

The goal of this scenario is to study the sealing ability of the cavity's closing system. This study is relevant in the evaluation of the sealing joint's relative maximum vertical displacement (fig. 5b). Sliding elements were not used for this scenario in order to allow the plug to separate itself from its support. Global plug stability is assured by horizontal supports situated on the exterior circumference of the plug, which are also taken into account in the simulation. The loading history is defined in figure 5f. The analysis covers a period of 40 years. The plug is assembled 1800 days after the end of the PCRV construction. Figures 6d, 6e and 6f show the evolution of relative displacements of the plug before applying pressure, t = 1980 days, after pressure applied, t = 1980 days and finally at the end of the power-station's life span, t = 14600 days.

As a main result, this scenario shows that the relative vertical displacement of the reactor vessel-plug increases by 50 % over the life span of the power-station. The maximum observed relative vertical displacement is of 3.47 mm. This scenario also illustrates the importance of when the plug's cotter was actually installed in relation to the completion of the power-station itself. The assembly at the last moment increases the relative vertical displacement of the reactor vessel-plug, for the prestress's creep within the vessel, having the tendancy to crush the plug, decreases over the alloted period of time.

4. CONCLUDING REMARKS

In this article we presented comparisons of finite element computations with experiments. Results show that simple nonlinear constitutive laws can encompass the main physical behaviour of reinforcement steel and concrete. Adjusting the parameters of these laws with

the help of classical experimental tests allows a qualitative and quantitative approach which shows good agreement with tests results on complex structures. Also long-term behaviour can be analysed which would'nt be possible experimentally.

REFERENCES

[1] HHT project reports Bonnard & Gardel SA Lausanne, 1975 - 1980.

[2] B. Saugy "Etude d'un modèle de déformation tridimensionnel non-linéaire pour le calcul à la rupture par éléments finis". Thèse No 323 (1979) Ecole Polytechnique Fédérale de Lausanne.

[3] Th. Zimmermann "Contribution à l'analyse non-linéaire des structures en béton armé et précontraint - Base d'un modèle rhéologique pour leur calcul par la méthode des éléments finis". Thèse No 253 (1976) Ecole Polytechnique Fédérale de Lausanne.

[4] B. Rebora, F. Uffer, Th. Zimmermann "Nonlinear analysis up to rupture of a model of a multicavity prestressed concrete pressure vessel". SMIRT IV, San Francisco, Paper H 3/4 (1977).

[5] R. Favre, M. Koprna, J.P. Jaccoud "Tests on model of a prestressed concrete nuclear pressure vessel with multiple cavities". SMIRT IV, San Francisco, Paper H 4/2 (1977).

[6] Th Zimmermann, B. Rebora "Three dimensional nonlinear dynamic analysis of reinforced concrete with the program 'TRIDI'. Constitutive model and algorithms". Internal report IENER N401.1D4 (1979).

[7] I.I. Ulitskii "A method of computing creep and shrinkage deformation of concrete for pratical purposes". Beton i Zhelezobeton No 4 (1962).

[8] C. Rodriguez, B. Rebora, J.D. Favrod "Model - Including thermal creep effects - for the analysis of three-dimensional concrete structures, comparison with tests". SMIRT V, Berlin, Paper H 4/8 (1979).

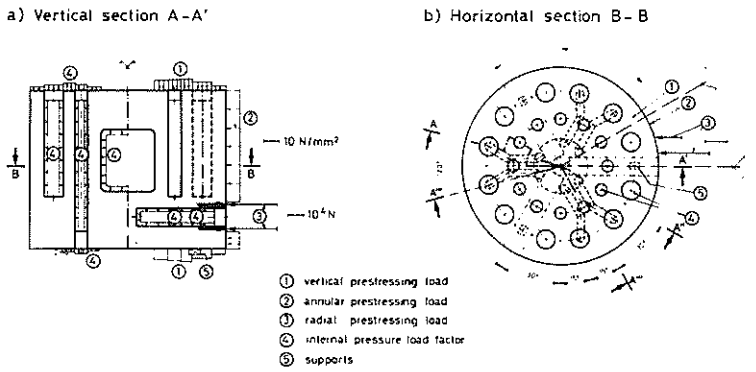

Fig. 1 : Geometry and loads of static rapid analysis

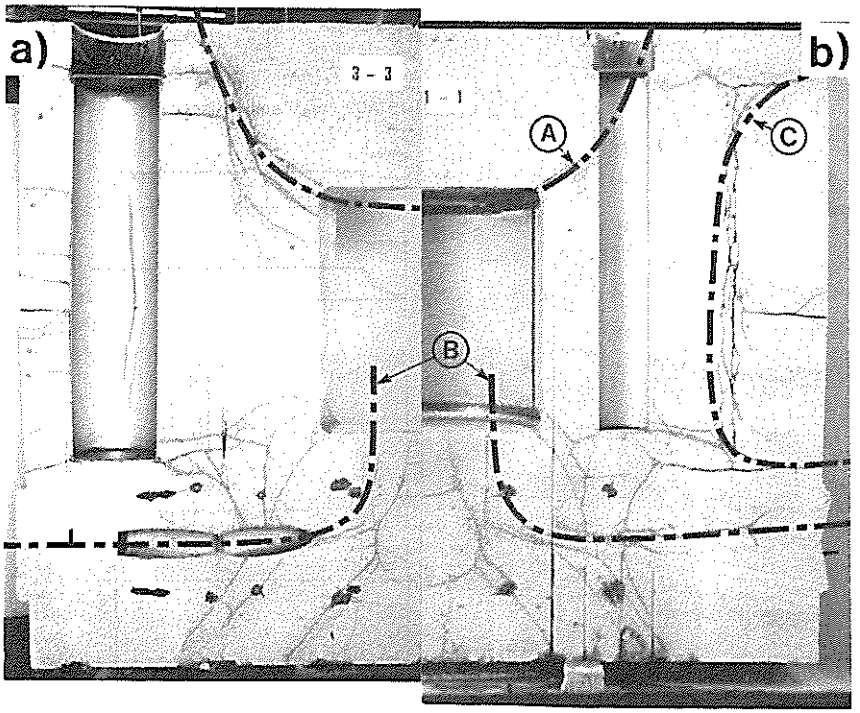

Fig. 2 : Post mortem experimental examination (section A''' - A''')
a) yielding of steel : liner
b) cracking schemes : concrete

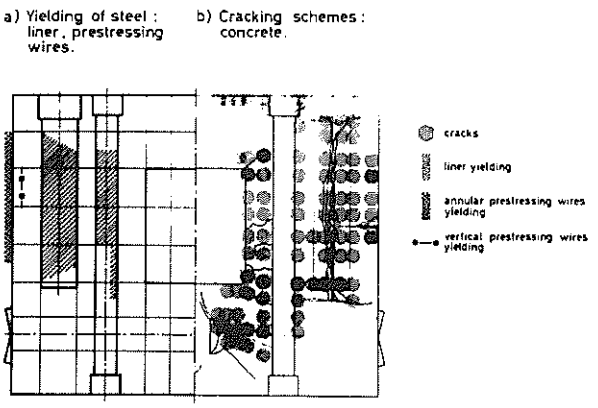

Fig. 3 : Post mortem numerical examination (section A - A'')

a) Thermal creep law

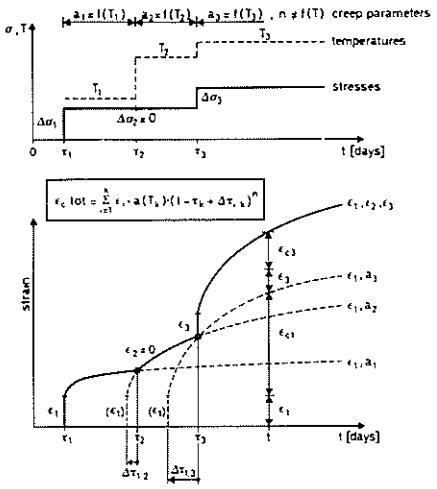

b) Mechanical properties

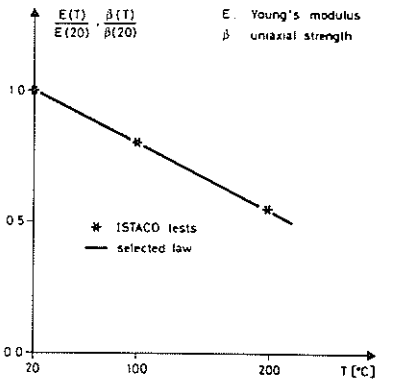

c) Creep and shrinkage parameters

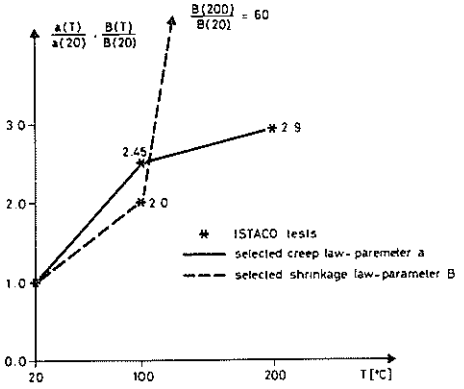

d) ISTACO test simulation

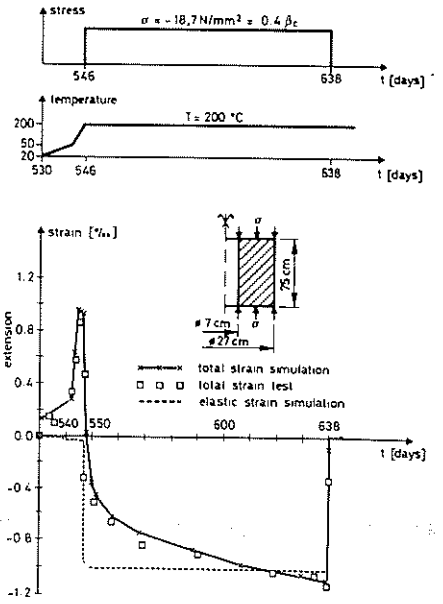

Fig. 4 : Concrete thermal laws

Materials \ Parameters	E N/mm²	ν	α °C⁻¹·10⁻⁶	a*	n*	B*	$c_s(\infty)$*	β_c N/mm²	β_t N/mm²
Concrete 20°C	40 000*	.2	8.	.22	.27	.006	-.0004	- 51*	5.1
Concrete 70°C	35 000*	.2	8.	.44	.27	.0098	-.0004	- 45*	4.5
Liner	200 000	.33	12.					-285.4	285.4
Support strut	160 600	.3	12.					-240.	240.
Sliding element	40 000	.2	8.						

* experimental , { } assumption

Table 1 : Material properties

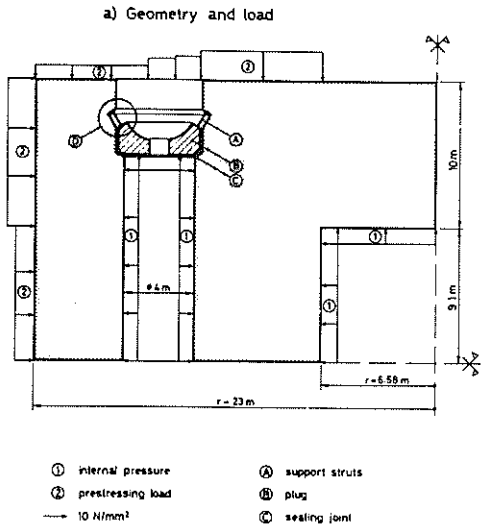

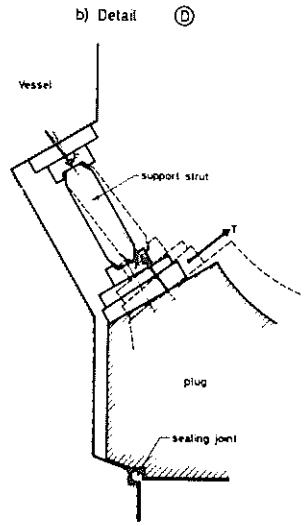

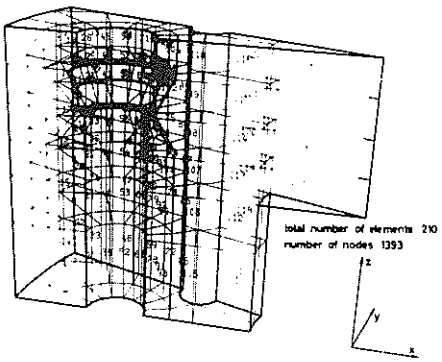

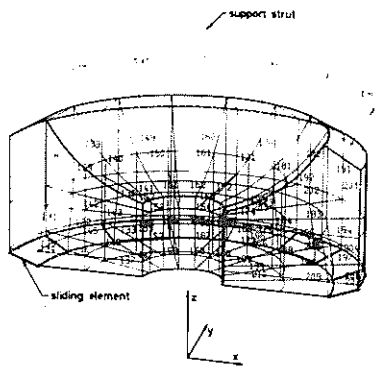

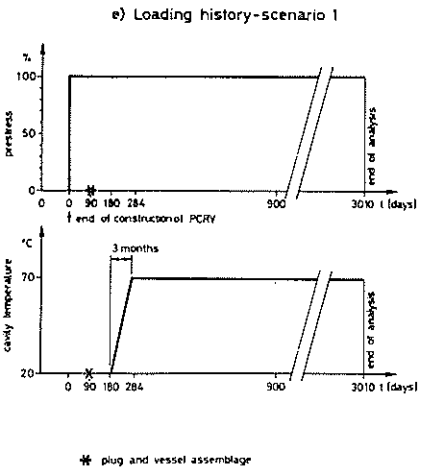

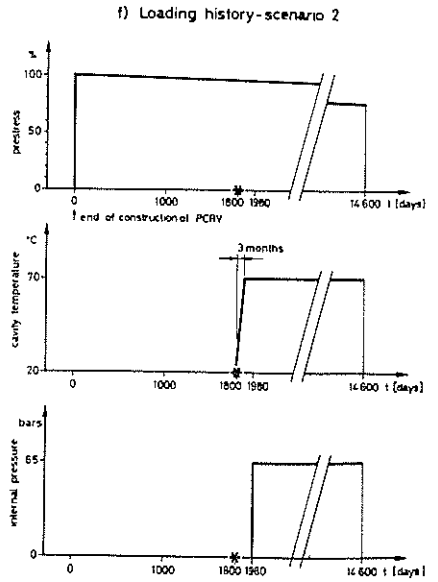

Fig. 5 : Geometry, mesh and loading historys of creep analyses

a) Scenario 1 - Stresses t = 284 days

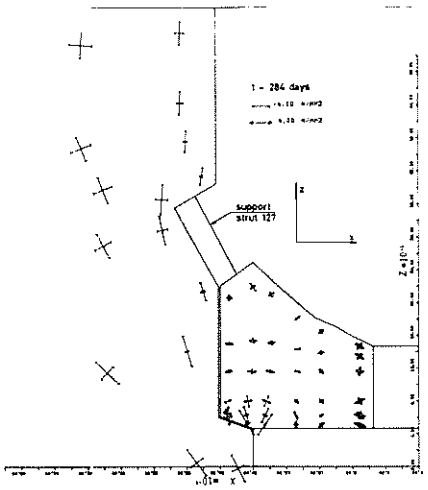

b) Scenario 1 - Stresses t = 3010 days

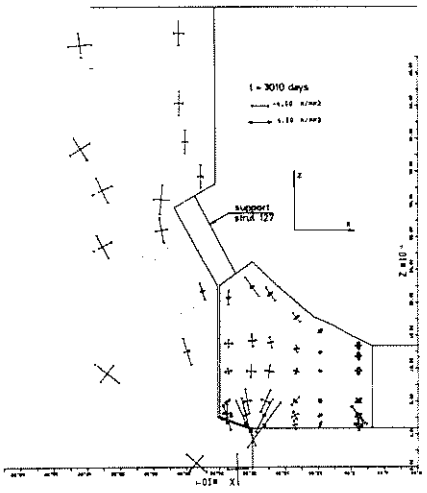

c) Scenario 1 - Stress-history in the support struts

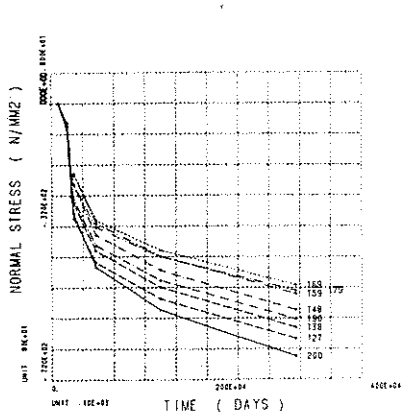

d) Scenario 2 - Relative displacements t = 1980 days

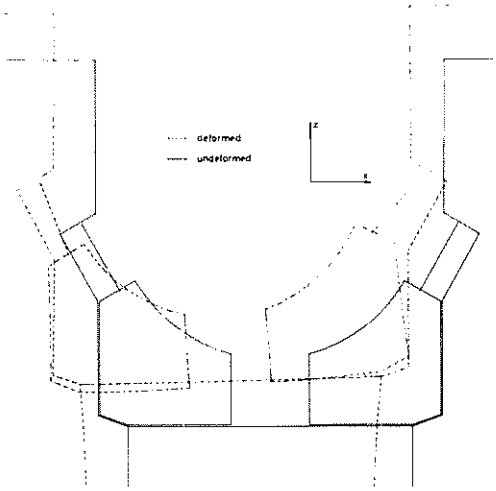

e) Scenario 2 - Relative displacements t = 1980 days

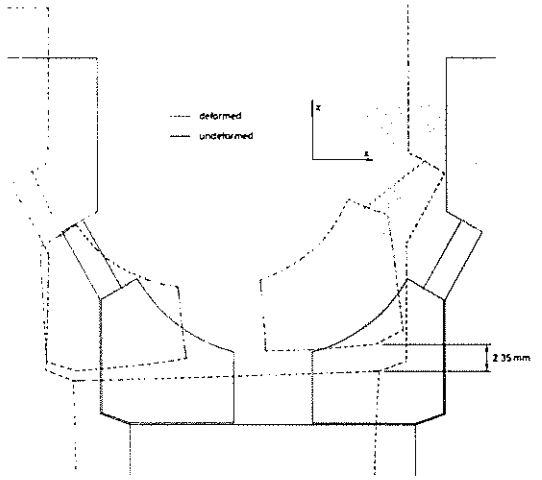

f) Scenario 2 - Relative displacements t = 14 600 days

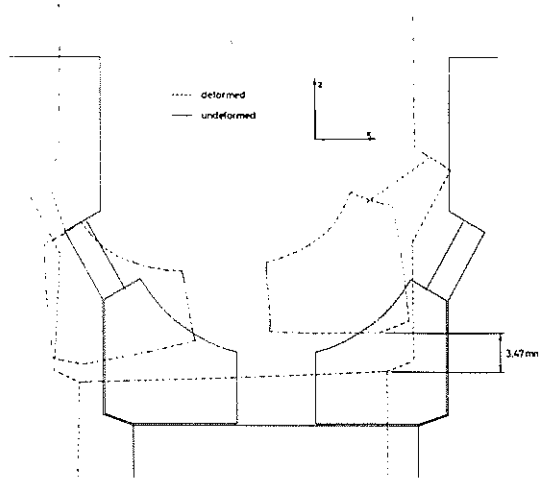

Fig. 6 : Main results of creep analyses